Experimental Investigation of an Automobile Air-Conditioning System using Integrated Brushless Direct Current Motor Rotary Compressor

M.F. Sukri[1,4,a], M.N. Musa[2], M.Y. Senawi[1] and H. Nasution[3]

[1]*Faculty of Mechanical Engineering, Universiti Teknologi Malaysia,81310 Johor Bahru, Johor, Malaysia*
[2]*UTM-Ocean Thermal Energy Center (UTM-OTEC), Universiti Teknologi Malaysia, Wilayah Persekutuan Kuala Lumpur, Jalan Semarak, 54100 Kuala Lumpur, Malaysia*
[3]*Automotive Development Centre, Universiti Teknologi Malaysia, 81310 Johor Bahru, Johor, Malaysia*
[4]*Efficient Energy & Thermal Management Research Group, Universiti Teknikal Malaysia Melaka, Hang Tuah Jaya, 76100 Durian Tunggal, Melaka*

Abstract. The present study presents an experimental investigation on the effect of condenser air inlet temperature and dimensionless parameter of X on the performance of automobile air-conditioning (AAC) system using integrated brushless direct current motor-rotary compressor and electronic expansion valve. The other components of AAC system are from original component of AAC system used for medium size passenger car. The experimental results showed that the increment of the condenser air inlet temperature and X caused an increase in condensing temperature, cooling capacity and compressor work, while decreasing the coefficient of performance (COP). Meanwhile, the evaporating temperature increase with the increment of condenser air inlet temperature, but decrease with decrement of X. In general, AAC system have to work at higher value of X in order to produce more cooling capacity, thereby increment in compressor work also occurs due to energy balance. However, at higher value of X, the COP of the system dropped due to dominant increase in compressor power, as opposed to a rise in cooling capacity. Due to this reason, the best operation of this compressor occurs at $X = 4.96$ for constant T_5 (35ºC), or at $T_5 = 30$ºC for constant X (4.96).

1 Introduction

An automotive air-conditioner is one of the most important accessories in typical land vehicles, which provides thermal comfort to the driver and passenger. Thermal comfort especially for drivers is crucial since road safety also improves with the comfort of the driver and a pleasant environment reduces driver fatigue [1]. However, automotive air-conditioning (AAC) system consumes second largest of energy after power train [2], thereby becoming a critical issue because of increasing concerns on energy cost, thermal comfort, greenhouse gas emissions, and vehicle performance.

Since the compressor consumes the highest amount of energy (65%) in a typical AAC system [3], a small improvement in compressor efficiency will leads to a larger reduction in power consumption. As a result, energy is consumed efficiently, and a significant improvement in the system performance is achieved. In the other aspect, reduction in energy consumption with more efficient compressor can decreases greenhouse gas emissions. This low-carbon technology is highly relevant in the real world and an important research interest related to energy-efficient systems. Many countries, particularly developed ones, have policies to reduce greenhouse gas emissions, especially at the transportation industry. Due to these reasons, numerous studies have been conducted to improve the AAC system performance using alternative compressor of conventional belt-driven fixed capacity compressor.

Tian et al. [4] highlighted that the compressor capacity control technique by using variable capacity compressor (VCC) has been used popularly in the AAC system due to its continuous operation, better thermal comfort inside car, and lower fuel consumption. Due to these reasons, Park et al. [3], Nasution and Wan Hassan [5], Qi et al. [6], Tian et al. [7] and Alkan and Hosoz [8] conducted few studies concerning AAC system equipped with VCC, particularly in the aspect of performance as compared to AAC system with fixed capacity compressor. In general, they found that AAC system with VCC yields better performance, less in exergy destruction and good thermal comfort sensation in the rapid changing environment with less energy usage/improved fuel consumption.

In different aspect, Ooi [9] optimized rotary compressor design and theoretically reduces mechanical losses by approximately 50% and improves the COP of the compressor by more than 14%. Later, a new gas compression mechanism called the “Revolving Vane” (RV) compressor was invented and theoretically shown to achieve improved mechanical, volumetric, and

[a] Corresponding author: mohdfirdaus@utem.edu.my

compression efficiencies compared with other existing compressor designs [10]. Further theoretical studies on this compressor have shown that friction, leakage, and discharge loss were substantially reduced in the new design, leading to significant improvements in efficiencies[10-12]. An experimental study at a shaft speed of 600–1200 rpm on the prototype of a RV compressor with air as the working fluid proved the reliability of the mechanism, achieving pressure ratios higher than 8:1 and more than 30 h of operation without any failure [13]. Further design improvements of the RV compressor with a fixed-vane significantly reduced the frictional losses by 18% to 41% and mechanical efficiency by 96% compared with the older RV compressor design [14].

Recently, Ekren et al. [15] demonstrated that direct current (DC) compressors have the potential to be used in energy-efficient refrigeration systems because these compressors do not require additional components such as a power inverter that an alternative current compressor would require. By utilizing this compressor, any problem related to the interaction of the refrigerant cycle components and the rapidly-changing operating conditions of the vehicle (speed, revolutions per minute, and so on) is solved. All types of ground vehicles are equipped with direct current batteries; thus, the authors agreed that efficient DC compressors are also among the best options to be used in an energy-efficient AAC system in future. One way of achieving an efficient DC refrigerant compressor is by integrating compressor pump with the latest brushless DC (BLDC) motor technology. The BLDC motors are microprocessor-controlled to keep the stator current in phase with the permanent magnets of the rotor, requiring less current for the same torque and therefore resulting in greater efficiency. Brushless DC motor has an excellent mechanical efficiency ranging from 85 to 90%. In addition, the BLDC motor-rotary compressor can be designed for low voltage (particularly 12V) up to high voltage of up to 300V. Hence, it is a better choice for powering an electric refrigerant compressor.

So far, however, research of AAC system coupled with BLDC motor-rotary compressor is very limited in the publication, at least to the author's knowledge. Therefore, it is the intent of this paper to investigate the performance of BLDC motor-rotary compressor available in the market, integrated with typical vapor compression refrigeration, AAC system.

2 Experimental set up

2.1 Design of experiment

The present study aims to investigate the correlation between the condenser air inlet temperature, condenser air face velocity, compressor speed and evaporator air volumetric flowrate to the performance of AAC system equipped with BLDC motor-rotary compressor and electronic expansion valve. The actual components of heat exchangers (evaporator and condenser), internal and external fans of 1.6L Proton Wira Aaeroback passenger car are used. A SIERRA06-0982Y3 high voltage BLDC variable speed hermetic compressor and electronic expansion valve (EEV) from Danfoss, model ETS 6 – 14 are used. The selection of these two components are based on vehicle compartment cooling load model proposed by Sukri et al. [16] for typical thermophysical data of 1.6L Proton Wira Aaeroback passenger car. Details of the selection process can be found in Sukri et al. [17]. The experimental test rig is mounted on an actual 1.6L Proton Wira Aeroback. Figure 1 shows the schematic diagram of the experimental test rig. Table 1 shows the model and accuracies of all test instruments.

Table 1. The accuracies of measuring instruments

Instruments	Measurements	Accuracies
T-Type Thermocouple with Pico TC-08 Data Logger	Refrigerant and air temperatures	±0.01°C
AKS 32 Danfoss Pressure Transducer	Refrigerant pressure	±0.01 bar
923 Fluke Air Velocity Meter	Air velocity	±0.01 m/s
Platon NGX Glass Flowmeter	Refrigerant mass flow rate	±1 g/s

The design of condenser ductwork is an open tunnel, rectangular shape and made of 20 mm thick insulation form (type insoform) with an overall length of 2870 mm. In order to provide a uniform air flow through the face of the condenser, air mixer and honey comb type air flow straightener were installed upstream of the condenser coil. The air sampling tube is constructed based on BS 5141-1:1975, Specification for Air Heating and Cooling Coils – Part 1: Method of Testing for Rating of Cooling Coils [18]. The frequency converter is used to control the condenser air face velocity. Meanwhile, the original evaporator ductwork of 1.6L Proton Wira Aeroback passenger car as in Figure 2 is utilized as experimental evaporator ductwork. The evaporator air volumetric flowrate is controlled by controlling the percentage of energy input supplied to the internal fan.

The condenser air face velocity profile is measured in the condenser ductwork with cross-sectional area of 500 mm x 500 mm at point 5 as in Figure 1. It is measured according to SAE International Surface Vehicle Standard 2008, Procedure for Measuring System COP of a Mobile Air Conditioning System on a Test Bench [19]. To obtain an averaged velocity, the readings have been taken by using a 923 Fluke hot-wire air velocity meter, placed successively at nine measuring points (at the same measuring plane). For each point, data is recorded for 5 minutes with averaged 10 seconds of sampling time. In total, 30 data is recorded for each point. The evaporator air volumetric flowrate is measured at point 7 as in Figure 1. At this point, the cross-sectional area of the original ductwork is 168 mm x 196 mm. The methodology adopted in measuring the averaged condenser air face velocity profile is also used in measuring averaged evaporator air velocity. The averaged evaporator air volumetric flowrate, V_7 is then calculated by multiplying

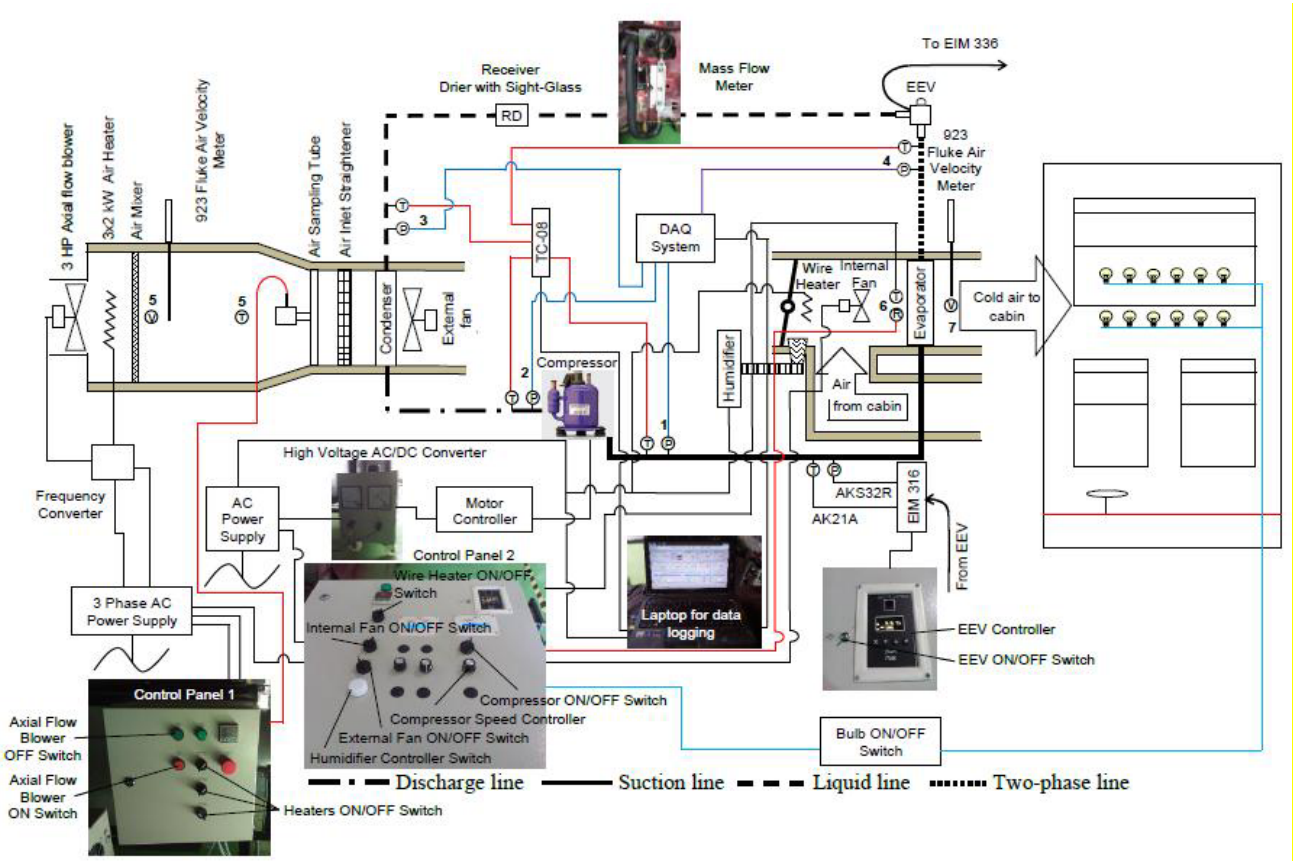

Figure 1. Schematic diagram of the experimental setup

the averaged evaporator air velocity, v_7 at point 7 with its cross-sectional area, thus:

$$V_7 = 0.032928 v_7 \quad (\mathrm{m^3/s}) \tag{1}$$

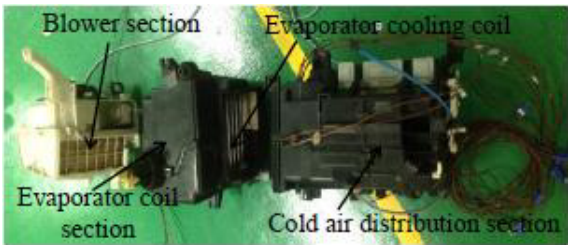

Figure 2. Evaporator ductwork

Since point sampling for each set of experimental work is time consuming, relationships are obtained between averaged condenser air face velocity and frequency of the inverter motor drive, and evaporator air volumetric flowrate with percentage of energy input. Simple linear regression are created using Microsoft Excel yields correlations as in Figure 3(a) and 3(b) for condenser and evaporator ductworks respectively. The subsequent experiments are conducted by setting an input frequency of the inverter motor drive and percentage of energy input, and the averaged air face velocity and averaged evaporator air volumetric flowrate are obtained from equations 2 and 3 respectively.

$$v_5 = 0.0896 f - 0.17 \,(\mathrm{m/s}) \tag{2}$$

$$V_7 = 5.9449 c + 7.6091 \,(\mathrm{m^3/h}) \tag{3}$$

2.2 Experimental Procedure

The experimental work is conducted in steady state condition. The tests is conducted by varying the value of dimensionless parameter, $X\left(V_7 {N_c}^2 / {v_5}^3\right)$ and condenser air inlet temperature, T_5 at constant value of evaporator air inlet temperature, T_6 (30ºC) and evaporator air inlet humidity ratio, ϕ_6 (50%). To stabilize the air-conditioning system, the system is run at least 20 minutes prior to each test before measured output variables are recorded as proposed by SAE International Surface Vehicle Standard 2008, Procedure for Measuring System COP of a Mobile Air Conditioning System on a Test Bench [19]. The output variables of refrigerant mass flow rate, $\dot{m}_r$, temperature and pressure at point 1 to 4 as in Figure 1 are recorded for ten minutes as proposed by SAE International Surface Vehicle Standard 2008, Procedure for Measuring System COP of a Mobile Air Conditioning System on a Test Bench [19]. The sampling time is 30 seconds. In total 20 data points is collected for each setting.

At each experimental setting, X is maintained at 4.96, 11.74 and 22.92 by controlling the value of N_c, v_5 and V_7 as in Table 2. At each value of X, T_5 is kept at 35ºC. Then, the experimental is repeated at T_5 of 30, 35 and 40ºC, but at constant value of X (11.74). During the entire experimental investigation, the ϕ_6 is maintained at 50% by controlling the humidifier manually. The EEV is also manually controlled at 100% of opening degree, and the input direct current voltage to the compressor is kept at 300 VDC.

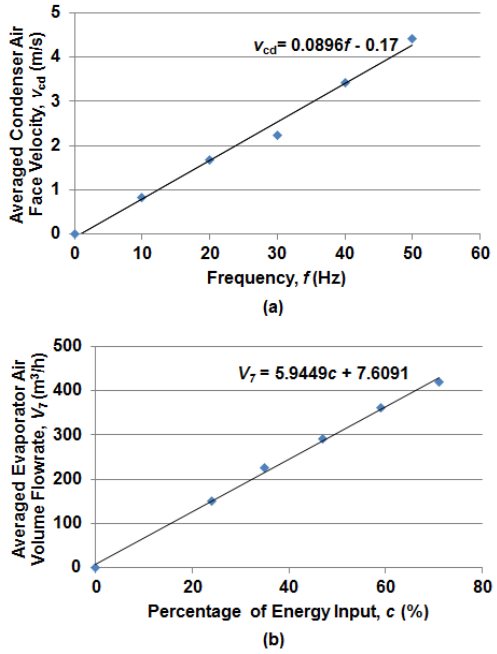

Figure 3. Liner regression between (a) averaged condenser air face velocity and frequency and (b) averaged evaporator air volumetric flowrate and percentage of energy input.

Table 2. The setting input variables during experimental work.

$X = \frac{V_7 N_c^{\,2}}{v_5^{\,3}}$	N_c (rpm)	V_7 (m³/h)	v_5 (m/s)
4.96	2300	190	2.5
11.74	3700	300	3.0
22.92	6500	450	4.0

The cooling capacity, Q_e and compressor work, W_c are calculated based on refrigerant enthalpy, h difference between inlet and outlet of the evaporator and compressor respectively, where:

$$Q_e = \dot{m}_r (h_1 - h_4) \quad (4)$$

$$W_c = \dot{m}_r (h_2 - h_1) \quad (5)$$

with , = 1, 2, 3, 4.

The coefficient of performance, COP is then determined as:

$$COP = Q_e / W_c \quad (6)$$

3 Results and discussion

The condensing temperature is higher at increased condenser air inlet temperature (Figure 4(a)) and X (Figure 4(b)). When the condenser air inlet temperature and the value of X are increased, the temperature of refrigerant discharged from the compressor will be higher cause an increased in condensing temperature. Simultaneously, the higher condensing temperature cause an increased in compressor work, as shown in Figure 5(a) and 5(b).

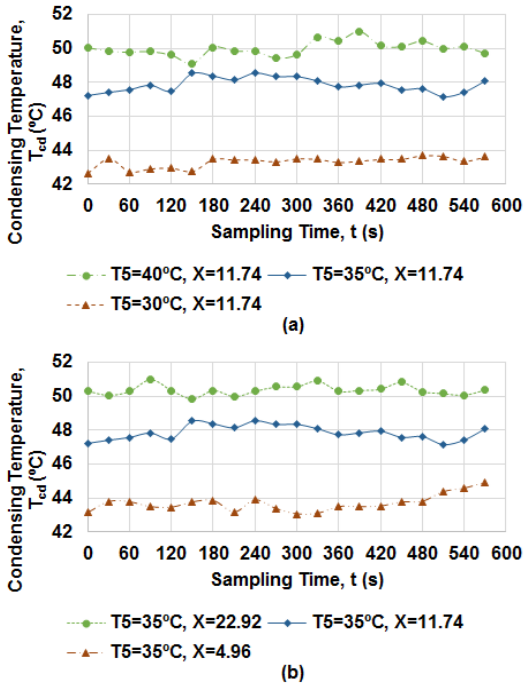

Figure 4. Condensing temperature over time (a) at constant X = 11.74 and (b) at constant condenser air inlet temperature, T_5 = 35ºC.

Figure 6(a) and 6(b) shows the effect of cooling capacity at different condenser air inlet temperature and X respectively. The decreases in the cooling capacity at lower condenser air inlet temperature as in Figure 6(a) could be due to decrease in the enthalpy difference in the evaporator caused by drop in evaporating temperature as in Figure 7(a). Therefore at constant value of X, the refrigeration capacity decreased with the decrement of evaporating temperature. However, Figure 6(b) and 7(b) show that at constant condenser air inlet temperature, the cooling capacity decreased with the increment of evaporating temperature. It can be clearly seen that for energy balance, at lower operating conditions of X (lower of compressor speed, evaporator air volumetric flowrate and condenser air face velocity), the system produces lower cooling capacity at high evaporating temperature.

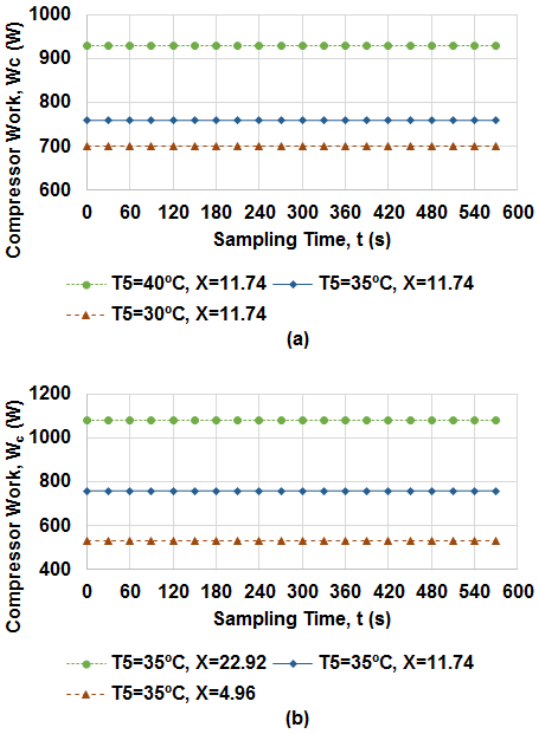

Figure 5. Compressor work over time (a) at constant X = 11.74 and (b) at different constant condenser air inlet temperature, T_5 = 35ºC.

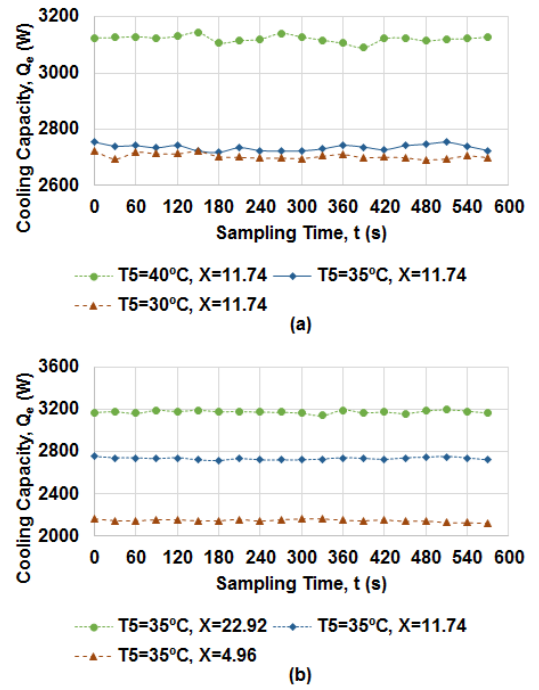

Figure 6. Cooling capacity over time (a) at constant X = 11.74 and (b) at different constant condenser air inlet temperature, T_5 = 35ºC.

Figure 8(a) and 8(b) show the relationship between the *COP* and condenser air inlet temperature at X of 11.74, and *COP* with X at condenser air inlet temperature of 35ºC respectively. It shows that the COP decrement is due to the increase in the condenser air inlet temperature and also with the increase of X. According to Eq. (6), the *COP* is influenced by the cooling capacity and compressor work. An increment in condenser air inlet temperature (Figure 5(a) and 6(a)) as well as in X (Figure 5(b) and 6(b)) causing increase in both, cooling capacity and compressor work. Hence, a dominant increase in compressor power, as opposed to a rise in cooling capacity lead to lower *COP* in both cases.

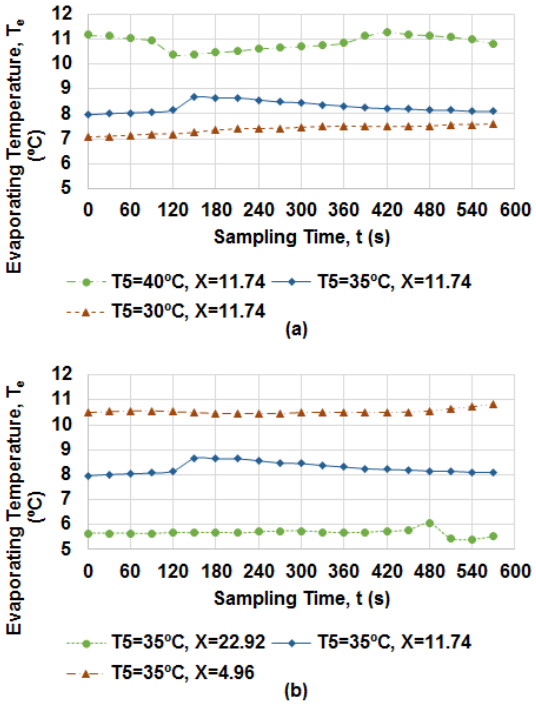

Figure 7. Evaporating temperature over time (a) at constant X = 11.74 and (b) at constant condenser air inlet temperature, T_5 = 35ºC.

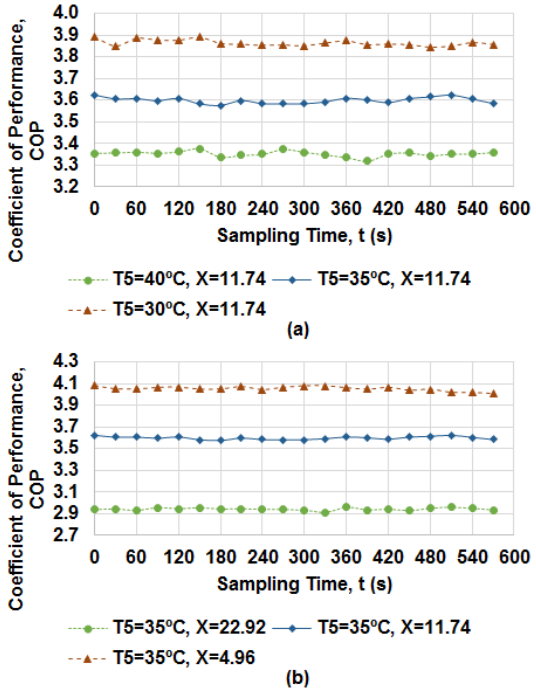

Figure 8. Coefficient of performance over time (a) at constant X = 11.74 and (b) at constant condenser air inlet temperature, T_5 = 35ºC.

4 Conclusions

The present study provides experimental result of an automobile air-conditioning system equipped with integrated BLDC motor-rotary compressor and EEV. The results of this study showed that the increment of the condenser air inlet temperature and value of X respectively caused an increase in condensing temperature, cooling capacity and compressor work, while decreasing the COP. However, the evaporating temperature increases with the increment of condenser air inlet temperature, but decrease with decrement of X. In general, AAC system have to work at higher value of X, particularly at high compressor speed in order to produce more cooling capacity, thereby increment in compressor work also occurs due to energy balance. However, at higher value of X, the COP of the system dropped due to dominant increase in compressor power, as opposed to a rise in cooling capacity. As a result, the best operation of this compressor occurs at X = 4.96 for constant T_5 (35ºC) or at T_5 = 30ºC for constant X (4.96).

Acknowledgements

The authors would like to be obliged to Universiti Teknologi Malaysia, Universiti Teknikal Malaysia Melaka and Ministry of Education Malaysia for providing laboratory facilities and all financial assistances, especially under project no. Q.J130000.2424.00G41.

References

1. M. Konz, *A generic simulation of energy consumption of automobile air conditioning systems* (M Tech Eng Thesis. Nelson Mandela Metropolitan University, 2007).
2. M.A. Roscher, W. Leidholdt, J. Trepte, Int J Elec Power **37**(1), 126-130 (2012).
3. S.K. Park, H. Kim, H. Ahn, H.S. Park, *SAE Technical Paper*, 2006-01-0164 (2006).
4. C. Tian, H. Xu, L. Zhang, X. Li, Appl Therm Eng **29**, 2824–2831 (2009).
5. H. Nasution, M.N. Wan Hassan, Clean Techn Environ Policy **8**, 105–111 (2006).
6. Z. Qi, J. Chen, Z. Chen, W. Hu, B. He, Appl Therm Eng. **27**, 927–933 (2007).
7. C. Tian, H. Xu, X. Li, Y. Liao Y. Appl Therm Eng. **27**, 1868–1875 (2007).
8. A. Alkan, M. Hosoz. Int J Refrig **33**(3), 487-495 (2010).
9. K.T. Ooi, Appl Therm Eng. **25**(5-6), 813–829 (2005).
10. Y.L. Teh, K.T. Ooi, Int J of Refrig **32**(5), 1092-1102 (2009).
11. Y.L. Teh, K.T. Ooi, Int J Refrig **32**(5), 1103-1111 (2009).
12. Y.L. Teh, K.T. Ooi, Int J Refrig **32**, 945-920 (2009)
13. Y.L. Teh, K.T. Ooi, Appl Therm Eng **29**(14-15), 3235–3245 (2009).
14. K.M. Tan, K.T. Ooi, Int J Refrig **34**(8), 1980-1988 (2011).
15. O. Ekren, S. Celik, B. Noble, R. Krauss, Int J Refrig **36**(3), 745-757 (2013).
16. M.F. Sukri, M.N. Musa, M.Y. Senawi, H. Nasution, *7th International Meeting on Advances In Thermofluids (7th IMAT)* (Swiss-Garden Hotel and Residences, Kuala Lumpur Malaysia, Nov 2014).
17. M.F. Sukri, M.N. Musa, K. Sumeru, S. Sodiya, JAMT **8**(2), 39-49 (2014).
18. BS 5141-1:1975, *Specification for Air Heating and Cooling Coils – Part 1: Method of Testing for Rating of Cooling Coils* (1975).
19. SAE International Surface Vehicle Standard, *Procedure for Measuring System COP of a Mobile Air Conditioning System on a Test Bench* (2008).